J. Phys. Chem. A **2003,** *107,* 7101−7105

On the Isotope Effect in F + HD Reaction at Ultracold Temperatures[†]

N. Balakrishnan*

Department of Chemistry, University of Nevada Las Vegas, 4505 Maryland Parkway,
Las Vegas, Nevada 89154

A. Dalgarno

Institute for Theoretical Atomic and Molecular Physics, Harvard-Smithsonian Center for Astrophysics,
60 Garden Street, Cambridge, Massachusetts 02138

Received: December 31, 2002; In Final Form: April 3, 2003

Isotope branching in the F + HD reaction is investigated at ultracold temperatures. It is found that in the limit of zero temperatures, the rate coefficient for HF formation in the F + HD ($v = 0$, $j = 0$) reaction is a factor of 5.5 greater than that of DF formation. The difference is attributed to the more efficient tunneling of the lighter atom. For HD molecules initially in the $j = 1$ excited rotational level, a clear preference is seen for chemical reaction leading to HF and DF products with an HF/DF branching ratio of 5.2 rather than for nonreactive rotational quenching.

I. Introduction

Several novel methods of creating ultracold molecules have been proposed recently,[1−4] and collisional properties of ultracold molecules have received considerable attention.[5−14] Coherent oscillations between atomic and molecular counterparts in Bose-Einstein condensates of ^{87}Rb atoms have been demonstrated by Wieman and co-workers,[15] and quantum collective effects leading to "superchemistry" in molecular BECs have been proposed.[16]

We have demonstrated[17] that exothermic chemical reactions may occur with significant rate coefficients at ultracold temperatures. Our study, applied to the hydrogen exchange reaction in the F + H_2 system, showed that the rate coefficient is finite in the limit of zero temperature in accordance with the Wigner law, with a magnitude of 1.25×10^{-12} cm^3 s^{-1}. The relatively large value of the limiting rate coefficient, despite an energy barrier of about 500 K in the entrance channel of the reaction, was attributed to tunneling and the long duration of the collision. More recently, Soldán et al.[18] have reported a rate coefficient of 5.2×10^{-10} cm^3 s^{-1} for the vibrational relaxation in spin-polarized $Na_2(v)$ + Na collisions for the $v = 1$ vibrational level in the zero-temperature limit. For the sodium trimer, the exchange reaction has no energy barrier and vibrational relaxation proceeds also via reactive scattering.

In this paper, we investigate the F + HD system at ultracold temperatures. The F + HD system is particularly interesting because it has two reactive channels corresponding to the HF and DF products. The F + H_2 system and its hydrogen isotopic constituents have served as benchmark systems for numerous experimental and theoretical investigations[19−37] of state-to-state reaction dynamics, and they continue to be a focus of attention because of the importance of resonances and quantum mechanical tunneling that dominate at energies below the barrier height of the reaction. We also explore competition between chemical reaction and nonreactive rotational quenching in rotationally excited HD molecules. Our results show that chemical reaction dominates in the limit of zero temperature.

The reactive scattering calculations were carried out using the ABC quantum scattering program of Skouteris et al.[38] and the potential energy surface (PES) developed for the F + H_2 system by Stark and Werner.[19] We neglect the fine-structure splitting in the F(^2P) atom because it has been shown[25,33] to have little effect on the reaction.

II. Results and Discussion

We report results for total angular momentum $J = 0$ and *s*-wave scattering in the incident channel for F + HD ($v = 0$, $j = 0$) collisions and $J = 1$ and *s*-wave scattering for F + HD ($v = 0, j = 1$) collisions. Contributions from higher partial waves vanish in the limit of zero energy. Because of the low collision energies involved and the small values of the reaction probabilities at low energies, convergence of the reaction probabilities at low energies is an important issue. Convergence has to be sought against the number of rovibrational levels in the basis set, the maximum value of the hyper radius $\rho_{\max}$, and the step size $\Delta\rho$. While converged reaction probabilities can be obtained at translational energies above 10^{-3} eV by using a step size of $\Delta\rho = 0.05$ au and a matching radius of $\rho_{\max} = 12$ au, smaller step-size and larger matching radius were needed at low energies. We have carried out extensive convergence tests as functions of all three parameters mentioned above.

Figure 1 illustrates the convergence of the total reaction probabilities with respect to $\rho_{\max}$ and $\Delta\rho$ for the HF product channel in F + HD ($v = 0, j = 0$) collisions for kinetic energies in the range 10^{-5}−10^{-3} eV. The reaction probabilities are converged to better than 1% in the entire energy range shown in Figure 1. A value of $\rho_{\max} = 25.0$ au and $\Delta\rho = 0.005$ au were found to be adequate to obtain converged results. A more sensitive test of convergence is the product rotational populations. Figure 2 shows the convergence of the rotational populations of the HF molecule with respect to the rovibrational basis set at an incident kinetic energy of 10^{-4} eV. Results are

---

[†] Part of the special issue "Donald J. Kouri Festschrift".

* Corresponding author. Fax: 702-895-4072. E-mail: naduvala@unlv.edu.

10.1021/jp022654v CCC: $25.00

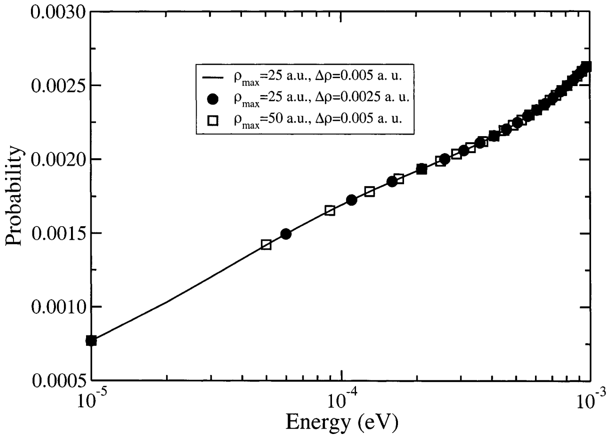

Figure 1. Reaction probabilities for HF formation in F + HD ($v = 0$, $j = 0$) collisions as functions of the incident kinetic energy corresponding to different values of ρ_{max} and $\Delta\rho$. Solid curve: $\rho_{max} = 25.0$ au and $\Delta\rho = 0.005$ au; filled circle: $\rho_{max} = 25.0$ au and $\Delta\rho = 0.0025$ au; open squares: $\rho_{max} = 50.0$ au and $\Delta\rho = 0.005$ au.

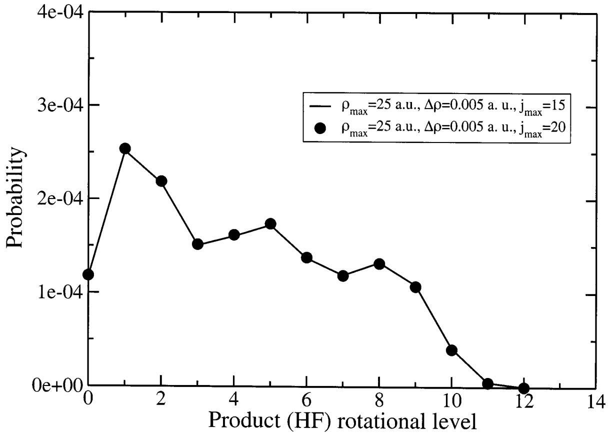

Figure 2. Reaction probabilities for HF ($v' = 2, j'$) formation in F + HD ($v = 0$, $j = 0$) collisions as functions of the product rotational quantum number at an incident kinetic energy of 1.0×10^{-3} eV. Results correspond to separate calculations with two different basis sets for the H_2 and HF rotational levels. Solid curve: $\rho_{max} = 25.0$ au, $\Delta\rho = 0.005$ au, $j_{max} = 15$; filled circle: $\rho_{max} = 25.0$ au, $\Delta\rho = 0.005$ au, $j_{max} = 20$.

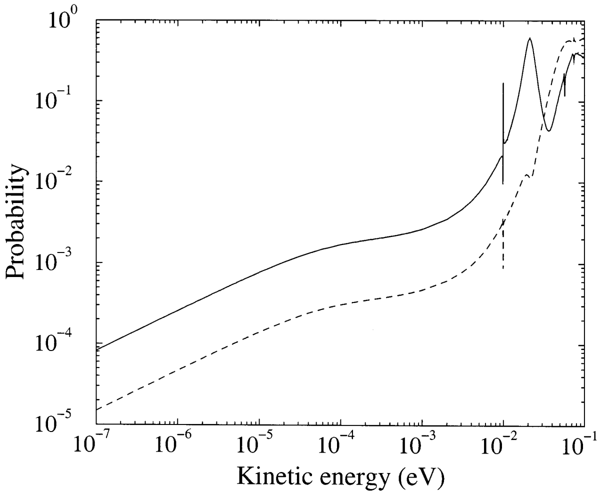

Figure 3. Total reaction probabilities for HF and DF formation in F + HD ($v = 0$, $j = 0$) collisions as functions of the incident kinetic energy: solid curve, HF product channel; broken curve, DF product channel.

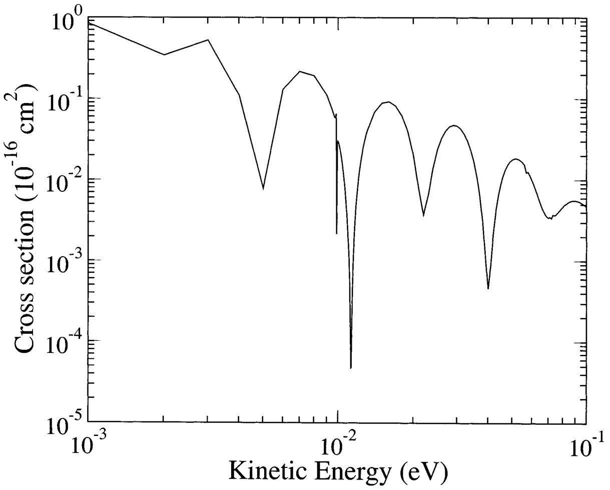

Figure 4. Elastic cross-sections for *s*-wave scattering in F + HD ($v = 0$, $j = 0$) collisions as functions of the incident kinetic energy. The sharp feature at 0.01 eV is a Feshbach resonance associated with the temporary formation of the F···HD ($v = 0$, $j = 1$) van der Waals complex during the collision.

shown from two calculations differing in the values of the cutoff energy (E_{max}) used in specifying the rovibrational levels of the diatomic fragments as well as the maximum value (j_{max}) of the diatomic rotational levels included in the calculations. The solid curve of Figure 2 corresponds to an E_{max} of 1.7 eV and j_{max} of 15, while the symbols correspond to a calculation with $E_{max} = 2.0$ eV and $j_{max} = 20$. For both calculations, ρ_{max} and $\Delta\rho$ were taken to be, respectively, 25.0 au and 0.005 au. The rotationally resolved probabilities are converged to within 5%. On the basis of these convergence tests, we have used $E_{max} = 1.7$ eV, $\rho_{max} = 25.0$ au, and $\Delta\rho = 0.005$ au in the calculations reported here.

Figure 3 presents the probabilities of HF and DF formation in F + HD ($v = 0$, $j = 0$) collisions over the energy range $10^{-7}-10^{-1}$ eV. The structures in the probabilities are due to resonances. The broad peak in the HF product centered at 0.02 eV has been considered in detail in a number of recent publications,[23,29−31,36] and it has been attributed to a reactive scattering resonance in the tunneling region. Here, we focus on features of the reaction at lower energies. The very sharp feature in the probability that occurs in both channels at about 0.01 eV is due to a Feshbach resonance associated with the temporary formation of a van der Waals complex F···HD ($j = 1$)[23,35] in the entrance channel of the reaction. It also appears in the elastic scattering cross-section as illustrated in Figure 4. The quasi-bound F···HD ($j = 1$) complex lies at 1.18×10^{-3} eV below the $j = 1$ threshold, and it can be accessed by scattering in the F + HD ($j = 0$) channel. The feature appears as a sharp peak in the HF product channel but as a dip in the DF channel and in the elastic scattering cross-section, reflecting the preferential dissociation of the F···HD ($j = 1$) complex by tunneling to the HF + D product channel. The probability for the HF product is 2 orders of magnitude greater than that of the DF product at the resonance energy. At incident energies lower than 10^{-6} eV, the Wigner law holds and the ratio of the probabilities for the two channels becomes constant. The limiting value of the HF/DF branching ratio at zero temperature is 5.5.

Direct measurements of the temperature dependence of the HF/DF branching ratio in the F + HD reaction have been reported by Persky.[39] The branching ratio was found to have a weak temperature dependence, and it varied from 1.55 at 159 K to 1.33 at 413 K. Using crossed molecular beam experiments, Dong et al.[32] reported cross-sections for F + H_2 and F + D_2 reactions at energies close to the reaction threshold. They

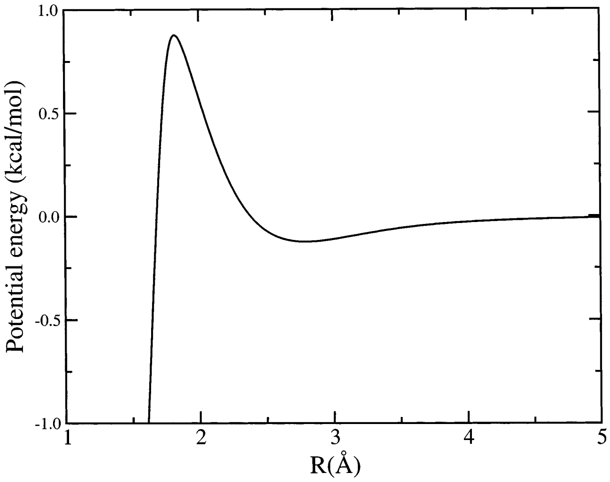

Figure 5. Adiabatic potential energy curve along the entrance channel of the F + HD reaction using the SW PES.

obtained branching ratios $\sigma_{n-H_2}/\sigma_{D_2}$ that remain flat at about 1.4 in the energy range 2.0 to 3.2 kcal/mol, rising to about 5.0 at an energy of 0.8 kcal/mol. Baer and co-workers[27,34] have explicitly calculated the branching ratio for the F + HD reaction in the temperature range of 100 to 500 K using the SW potential surface. They found a strong temperature dependence of the branching ratio with a value of about 1.5 at 450 K, close to the measured value of 1.4, and a value of about 6.0 at 100 K. Thus, the limiting value of the HF/DF product branching ratio from our calculations is consistent with available experimental and theoretical results at low temperatures.

The Stark-Werner potential has an energy barrier of 0.0629 eV (1.45 kcal/mol),[19] and at low energies the reaction occurs mainly through tunneling. The probability of tunneling is determined by the height and width of the barrier. The finite value of the branching ratio between the two channels may be understood by examining the transmission coefficients for H and D atom tunneling through a one-dimensional potential barrier. For this, we use the barrier height of the lowest adiabatic potential in the entrance channel of the F + HD reaction instead of the saddle point energy. The adiabatic potential includes zero-point energy along the reaction coordinate, and it is given by[21]

$$V(R) = \langle \chi_{v=0,\,j=0} | V(R, r, \theta) | \chi_{v=0,\,j=0} \rangle \qquad (1)$$

where $\chi_{v=0,j=0}$ is the lowest adiabatic rovibrational wave function of the F−HD system at a given value of the atom−molecule center-of-mass separation R, and $V(R, r, \theta)$ is the full potential energy surface. The lowest adiabatic potential for the F−HD system is shown in Figure 5 as a function of R. It has an energy barrier of 0.038 eV (0.88 kcal/mol) and a width of 0.35 Å (0.66 au), in close agreement with the values reported by Rosenman et al.[21] for the F + H_2 reaction on the same PES.

For simplicity, we consider tunneling through a rectangular potential barrier of height V_0 and width L, and a more realistic potential of $V(x) = V_0/(\cosh^2(\alpha x))$ where α determines the width of the barrier. V_0 for both potentials was taken to be 0.038 eV, the barrier height of the adiabatic potential shown in Figure 5. The width of the rectangular barrier was taken to be 0.35 Å, and the parameter α of $V(x)$ was taken to be 5.0 Å^{-1} so that it has a full width at half-maximum of about 0.35 Å. Transmission coefficients were calculated from analytical formulas[40] for the two potentials with appropriate masses for the H and D atoms. The ratios of the transmission coefficients for H and D atom tunneling through the two potentials and the HF/DF branching ratio are shown in Figure 6. At energies lower than 10^{-4} eV, the transmission coefficient ratios and the branching ratios approach finite limiting values. The limiting values of the ratios of H/D transmission coefficients for the rectangular barrier and $V(x)$ are 3.72 and 6.33 compared to an HF/DF branching ratio of 5.5. The qualitative differences in the computed HF/DF branching ratio at energies above 10^{-3} eV are due to details of the dynamics which are not captured by the simplified model. The overall agreement, especially with the more realistic barrier potential $V(x)$, supports the tunneling hypothesis.

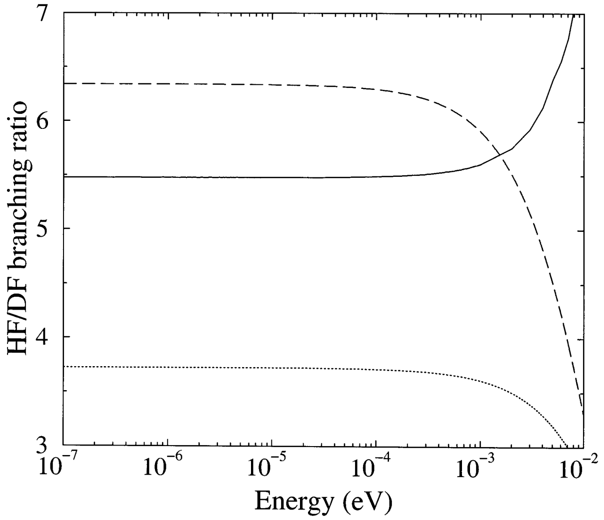

Figure 6. Branching ratio HF/DF for the F + HD (v = 0, j = 0) reaction as a function of the incident kinetic energy. Solid curve: results of quantum mechanical calculations; dashed curve: ratio of H/D transmission coefficients for tunneling through a potential barrier of the type $V(x) = V_0/\cosh^2(\alpha x)$; dotted curve: ratio of H/D transmission coefficients for tunneling through rectangular potential barrier.

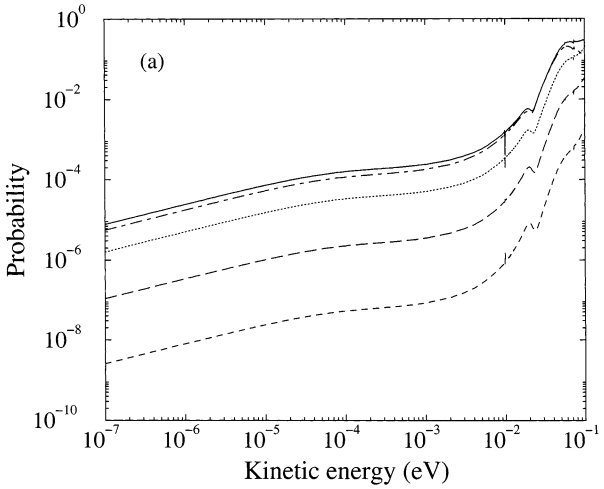

Figure 7. Vibrational distribution of DF(v') in F + HD (v = 0, j = 0) reaction as a function of the incident kinetic energy. Short-dashed curve: v' = 0; long-dashed curve: v' = 1; dotted curve: v' = 2; solid curve: v' = 3; dot−dashed curve: v' = 4.

Figure 7 shows the probabilities for DF formation in the various open vibrational levels as functions of the incident energy. The most populated levels are v = 3 and 4, and the relative populations of the vibrational levels remain unchanged at energies below 0.01 eV. Similar results for HF are shown in Figure 8. The first three vibrational levels are open at zero energy, and the v = 3 level becomes open at 0.071 eV. The most populated level is v = 2, which is about an order of magnitude more probable than the v = 1 level.

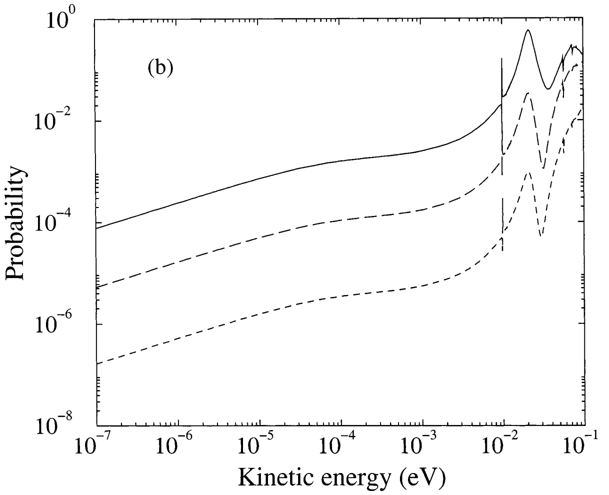

Figure 8. Same as in Figure 4 but for the HF(v') products. Short-dashed curve: $v' = 0$; long-dashed curve: $v' = 1$; solid curve: $v' = 2$.

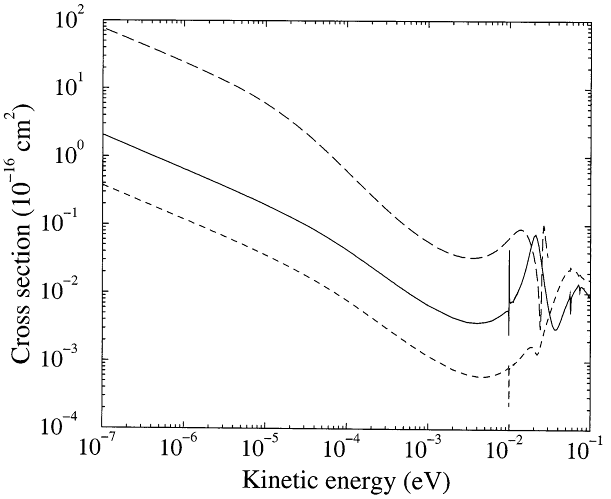

Figure 9. Comparison of *s*-wave cross-sections for the F + H_2 ($v = 0$, $j = 0$) and F + HD ($v = 0$, $j = 0$) reactions as functions of the incident kinetic energy. Short-dashed curve: DF product channel in F + HD reaction; solid curve: HF product channel in F + HD reaction; long-dashed curve: F + H_2 reaction.

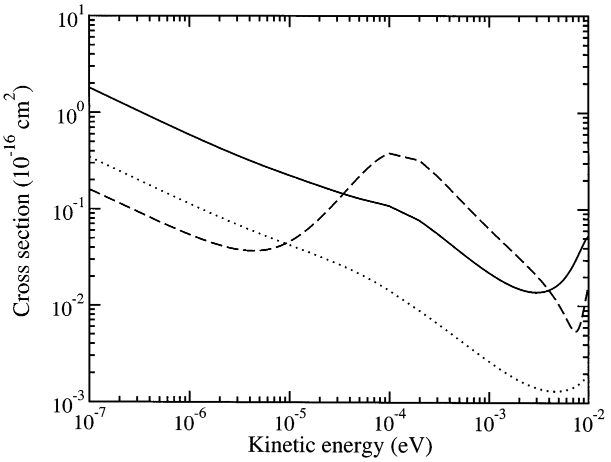

Figure 10. Comparison of cross-sections for HF and DF formation as well as nonreactive rotational quenching in F + HD ($v = 0$, $j = 1$) collisions for $J = 1$. Dotted curve: DF product channel; solid curve: HF product channel; long-dashed curve: nonreactive rotational quenching.

In Figure 9, we compare the $J = 0$ cross-sections for HF and DF products in the F + HD reaction with those for the F + H_2 reaction.[17] At energies below 10^{-6} eV, the cross-sections attain the Wigner limit, where they vary inversely as the velocity and the corresponding rate coefficients become finite. The cross-sections are comparable at energies above 0.02 eV. In the Wigner regime, the cross-sections are smaller by a factor of 35 for the F + HD reaction compared to those of the F + H_2 reaction. Rate coefficients are obtained by multiplying the cross-section with the relative velocity. The SW potential does not account for spin−orbit splitting of the fluorine atom into the $^2P_{3/2}$ and $^2P_{1/2}$ components. To account for the effect of multiple potential energy surfaces resulting from spin−orbit splitting,[22,41,42] the rate coefficients computed on the SW potential need to be multiplied with an electronic partition function of $(2 + \exp(-\Delta/k_BT))^{-1}$, where $\Delta = 50.1$ meV is the $^2P_{1/2}-^2P_{3/2}$ spin−orbit splitting in the fluorine atom, k_B is the Boltzmann constant, and T is the temperature in Kelvin. In the limit of zero temperature this becomes 1/2, and the rate coefficients reported below for F + HD and F + H_2 reactions are scaled by this factor. We obtain a zero-temperature limiting value of 3.3×10^{-14} cm^3 s^{-1} for the coefficient for the F + HD ($v = 0$, $j = 0$) reaction compared to 1.25×10^{-12} cm^3 s^{-1} for the F + H_2 reaction.[17]

We have also examined the competition between chemical reactivity and nonreactive rotational quenching at ultracold temperatures by investigating the F + HD ($v = 0$, $j = 1$) collisions. This required calculations for $J = 1$, which corresponds to *s*-wave scattering in the incident channel at ultralow energies. The $J = 1$ cross-sections for HF and DF products as well as inelastic rotational quenching are shown in Figure 10. The limiting value of the reactive cross-section is an order of magnitude larger than that of rotational quenching. This is in contrast to the F + D_2 system for which Bodo et al.[11] found that the rotational quenching dominates chemical reaction in F + D_2 $v = 0$, $j = 2$) collisions at low energies. The difference is attributed to the more efficient tunneling of the lighter H-atom. The limiting value of the HF/DF branching for F + HD ($v = 0$, $j = 1$) is estimated to be 5.2 compared to 5.5 for F + HD ($v = 0$, $j = 0$). Our finding that chemical reaction may dominate over rotational quenching will be of particular interest to future experiments on chemical reactivity in ultracold molecules.

Acknowledgment. This work was supported in part by a grant from the National Science Foundation (N.B.) and by the Chemical Sciences, Geosciences and Biosciences Division of the Office of Basic Energy Sciences, Office of Science, U.S. Department of Energy (A.D.). We thank Prof. Michael Baer for useful comments on an earlier version of the manuscript.

Note Added after ASAP Posting. This article was released ASAP on 5/01/2003. The fourth paragraph of the Results and Discussion section and reference 39 have since been updated. This updated version was posted on 07/21/2003.

References and Notes

(1) Weinstein, J. D.; deCarvalho, R.; Guillet, T.; Friedrich, B.; Doyle, J. M. *Nature* **1998**, *395*, 148.

(2) Bahns, J. T.; Stwalley, W. C.; Gould, P. L. *J. Chem. Phys.* **1996**, *104*, 9689.

(3) Bethlem, H. L.; Berden, G.; Crompvoets, F. M. H.; Jongma, R. T.; van Roij, A. J. A.; Meijer, G. *Nature* **2000**, *406*, 491.

(4) Wynar, R.; Freeland, R. S.; Han, D. J.; Ryu, C.; Heinzen, D. *Science* **2000**, *287*, 1016.

(5) Balakrishnan, N.; Forrey, R. C.; Dalgarno, A. *Phys. Rev. Lett.* **1998**, *80*, 3224.
(6) Balakrishnan, N.; Dalgarno, A.; Forrey, R. C. *J. Chem. Phys.* **2000**, *113*, 621.
(7) Balakrishnan, N.; Dalgarno, A. *J. Phys. Chem.* **2001**, *105*, 2348.
(8) Siska, P. E. *J. Chem. Phys.* **2001**, *115*, 4527.
(9) Avdeenkov, A. V.; Bohn, J. L. *Phys. Rev. A* **2001**, *64*, 052703.
(10) Bodo, E.; Gianturco, F. A.; Dalgarno, A. *J. Chem. Phys.* **2002**, *116*, 9222.
(11) Bodo, E.; Gianturco, F. A.; Dalgarno, A. *J. Phys. B: At. Mol. Opt. Phys.* **2002**, *35*, 2391.
(12) Flasher, J. C.; Forrey, R. C. *Phys. Rev. A* **2002**, *65*, 032710.
(13) Volpi, A.; Bohn, J. L. *Phys. Rev. A* **2002**, *65*, 052712.
(14) Balakrishnan, N.; Groenenboom, G. C.; Krems, R. V.; Dalgarno, A. *J. Chem. Phys.* **2003**, *118*, 7386.
(15) Donley, E. A.; Claussen, N. R.; Thompson, S. T.; Wieman, C. E. *Nature* **2002**, *417*, 529.
(16) Heinzen, D. J.; Wynar, R.; Drummond, P. D.; Kheruntsyan, K. V. *Phys. Rev. Lett.* **2000**, *84*, 5029.
(17) Balakrishnan, N.; Dalgarno, A. *Chem. Phys. Lett.* **2002**, *341*, 652; Balakrishnan, N.; Dalgarno, A. *Chem. Phys. Lett.* **2002**, *351*, 159.
(18) Soldán, P.; Cvitaš, M. T.; Hutson, J. M.; Honvault, P.; Launay, J.-M. *Phys. Rev. Lett.* **2002**, *89*, 153201.
(19) Stark, K.; Werner, H.-J. *J. Chem. Phys.* **1996**, *104*, 6515.
(20) Castillo, J. F.; Manolopoulos, D. E.; Stark, K.; Werner, H.-J. *J. Chem. Phys.* **1996**, *104*, 6531.
(21) Rosenman, E.; Hochman-Kowal, S.; Persky, A.; Baer, M. *Chem. Phys. Lett.* **1996**, *257*, 421.
(22) Manolopoulos, D. E. *J. Chem. Soc., Faraday Trans.* **1997**, *93*, 673.
(23) Takayanagi, T.; Kurosaki, Y. *J. Chem. Phys.* **1998**, *109*, 8929.
(24) Castillo, J. F.; Hartke, B.; Werner, H.-J.; Aoiz, F. J.; Bañares, L.; Martínez-Haya, B. *J. Chem. Phys.* **1998**, *109*, 7224.
(25) Alexander, M. H.; Manolopoulos, D. E.; Werner, H.-J. *J. Chem. Phys.* **1998**, *113*, 5710.
(26) Baer, M.; Faubel, M.; Martínez-Haya, B.; Rusin, L.; Tappe, U.; Toennies, J. P. *J. Chem. Phys.* **1999**, *110*, 10231.
(27) Baer, M. *Chem. Phys. Lett.* **1999**, *312*, 203.
(28) Aoiz, F. J.; Bañares, L.; Castillo, J. F. *J. Chem. Phys.* **1999**, *111*, 4013.
(29) Castillo, J. F.; Manolopoulos, D. E. *Faraday Discuss.* **1998**, *110*, 119.
(30) Skodje, R. T.; Skouteris, D.; Manolopoulos, D. E.; Lee, S.-H.; Dong, F.; Liu, K. *Phys. Rev. Lett.* **2000**, *85*, 1206.
(31) Skodje, R. T.; Skouteris, D.; Manolopoulos, D.; Lee, S.-H.; Dong, F.; Liu, K. *J. Chem. Phys.* **2000**, *112*, 4536.
(32) Dong, F.; Lee, S.-H.; Liu, K. *J. Chem. Phys.* **2000**, *113*, 3633.
(33) Alexander, M. H.; Manolopoulos, D. E.; Werner, H.-J. *J. Chem. Phys.* **2000**, *113*, 11084.
(34) Zhang, D. H.; Lee, S.-Y.; Baer, M. *J. Chem. Phys.* **2000**, *112*, 9802.
(35) Takayanagi, T.; Wada, A. *Chem. Phys. Lett.* **2001**, *338*, 195.
(36) Lee, S.-H.; Dong, F.; Liu, K. *J. Chem. Phys.* **2002**, *116*, 7839.
(37) Krems, R.; Dalgarno, A. *J. Chem. Phys.* **2002**, *117*, 118.
(38) Skouteris, D.; Castillo, J. F.; Manolopoulos, D. E. *Comput. Phys. Commun.* **2000**, *133*, 128.
(39) Persky, A. *J. Chem. Phys.* **1973**, *59*, 5578.
(40) Landau, L. D.; Lifshitz, E. F. *Quantum Mechanics (Nonrelativistic Theory)*; Pergamon: New York, 1977.
(41) Truhlar, D. G. *J. Chem. Phys.* **1972**, *56*, 3189.
(42) Truhlar, D. G. *J. Chem. Phys.* **1974**, *61*, 440E.